

# Automatic classification of in-vivo distal lung images for computer-aided diagnosis

Caroline Petitjean<sup>a\*</sup>, Chesner Désir<sup>a</sup>, Mathieu Salaün<sup>b</sup>, Luc Thiberville<sup>b</sup>, Laurent Heutte<sup>a</sup>

<sup>a</sup>Université de Rouen, LITIS EA 4108, BP 12, 76801 Saint-Etienne-du-Rouvray, France

<sup>b</sup>Clinique Pneumologique, Rouen University Hospital, LITIS EA 4108, 76031 Rouen, France

## Abstract.

*Until recently, the alveolar region could not be investigated in vivo. A novel technique, based on confocal microscopy, can now provide new images of the respiratory alveolar system, for which quantitative analysis tools must be developed, for diagnosis and follow up of pathological situations. In particular, we wish to aid the clinician by developing a computer-aided diagnosis system, able to discriminate between healthy and pathological subjects. This paper describes this system, in which images are first characterized through a 120-feature vector then classified by a Support Vector Machine (SVM). Experiments conducted on smoker and non smoker images show that the dimensionality of the feature vector can be reduced without decreasing significantly classification accuracy, and thus gaining some insight about the usefulness of features for medical diagnosis. These promising results allow us to consider interesting perspectives for this very challenging medical application.*

## 1 Introduction

The lungs are divided into two anatomic and functional regions: (i) the air conduction system, that includes the trachea, bronchi, and bronchioles, and (ii) the gas-exchange region, made of alveolar sacs. These sacs are made up of clusters of alveoli, tightly wrapped in blood vessels, that allow for gas exchange. Whereas the conduction airways can be explored in vivo during bronchoscopy, the alveolar region was until recently unreachable for in vivo morphological investigation. Therefore, the pathology of the distal lung is currently assessed only in vitro, using invasive techniques such as open lung biopsies. No real time imaging was available.

Recently, a new endoscopic technique, called Fibered Confocal Fluorescence Microscopy (FCFM), has been developed that enables the visualisation of the more distal regions of the lungs in vivo [7]. The technique is based on the principle of fluorescence confocal microscopy, where the microscope objective is replaced by a fiberoptic miniprobe, made of thousands of fiber cores. The miniprobe can be introduced into the 2 mm working channel of a flexible bronchoscope to produce in vivo endomicroscopic imaging of the human respiratory tract in real time. Real-time alveolar images are continuously recorded during the procedure and stored for further analysis. This very promising technique could replace lung biopsy in the future and might prove to be helpful in a large variety of diseases, including interstitial lung diseases [8].

In this context, a clinical trial is currently being conducted that collects FCFM images in several pathological conditions of the distal lungs and on healthy smoker and non-smoker volunteers. The images are selected from the in-vivo alveoscopy database by two medical experts. By definition, we exclusively term normal the images obtained from the healthy volunteer group. Images classified as pathological are selected from the image database only if (i) they were obtained from a patient with PID and (ii) the image was obtained from a lung segment that appeared abnormal on the chest CT Scan. FCFM images represent the alveolar structure, made of elastin fiber (Figure 1), with an approximate resolution of 1  $\mu\text{m}$  per pixel. This structure appears as a network of (almost) continuous lines. This elastic fiber framework can be altered by distal lung pathologies and as one can see on Figure 1, images acquired on pathological subjects differ from the ones acquired on healthy subjects.

The great complexity of these new images justifies the development of reproducible software tools for computer aided diagnosis, that enables automatic image description for diagnosis and follow up of pathological situations. The aim of the study is to conceive and develop methods for automatic analysis of FCFM images, so as to discriminate healthy cases from pathological cases. Since the images recorded within the alveolar regions of the lungs have not been very well described so far, we also wish to provide the clinician some insight about image characteristics that can help the diagnosis. In order to perform analysis and classification, the system relies on 188 annotated images acquired during the clinical trial, coming from both healthy (93) and pathological (95) cases. These latter cases include diverse interstitial pathologies: fibrosis, histiocytosis, proteinosis, systemic sclerosis and sarcoidosis.

---

\*Caroline.Petitjean@univ-rouen.fr

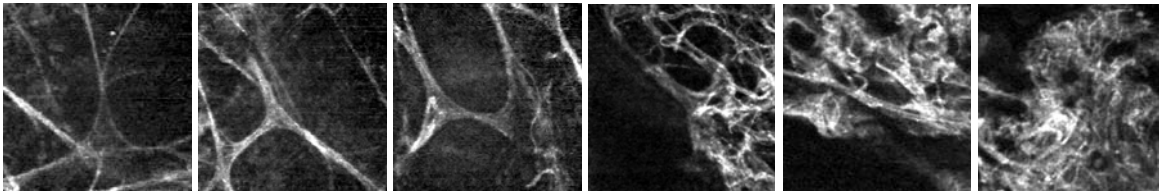


**Figure 1.** FCFM images of three healthy cases (left) and three pathological cases (right)

The remaining of this paper is organized as follows: our classification method is described in Section 2, and results and discussion are provided in Section 3. Section 4 concludes and draws some perspectives for this work.

## 2 Image classification method

As usual in data classification methods, our system includes a feature extraction step and a classification step [3].

### 2.1 Feature extraction

Features must be chosen to allow the discrimination between healthy and pathological subjects. As shown in Figure 2, some images present difficulties where pathological cases can be visually misclassified for healthy ones and vice versa. Because of the novelty of the images and the visual misclassification possibilities, the choice of features is critical.

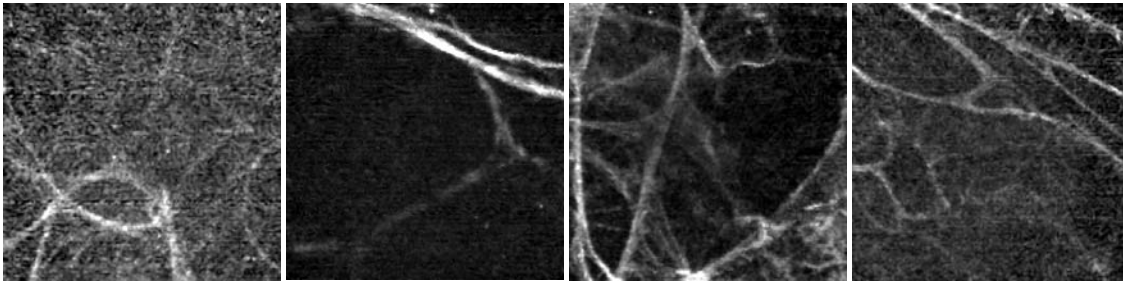


**Figure 2.** Difficult cases in FCFM images: two healthy subjects (left) and two pathological subjects (right)

Several general characteristics can be observed from the visual analysis of the images. As shown in Figure 1, the alveolar structure in healthy subjects can be described as contrasted continuous lines and curves. On the opposite, in the pathological subset, the disorganization of the meshing is illustrated by the numerous irregularities and the tangle of the fibered structures. Differences are mostly visible for the structure shape, image texture and contrast implying that numerical features must therefore be chosen among the ones that best describe the visual differences from these three points of view.

The **structure contrast** can be characterized by studying first order pixel gray level distribution and computing pixel densities. Because structures also show local differences, local parameters are computed on subwindows of the image. Subwindows are obtained by dividing by 4 the image height and width (Figure 3). Features characterizing the image contrast are (i) first order statistics on global and local histogram: mean, variance, skewness, kurtosis, entropy, (ii) global and local pixel densities obtained on binarized images using Otsu thresholding, (iii) the sum of the image gradient values, obtained using Prewitt operator. We could suppose that pathological images will have high values for densities, since a large number of pixels having high value cover a large part of the image.

The **complexity of the structure shape** can be characterized by studying the image skeleton. After skeletonization [2] obtained on the binary image, the number of junction points is computed. One can suppose that on clearly organized, healthy images, this number will be small, contrary to pathological images where the meshing mess will induce a higher number of points.

The **image texture** can be characterized by Haralick parameters computed from cooccurrence matrix [5]: energy, contrast, homogeneity, correlation, along 4 directions ( $0^\circ$ ,  $45^\circ$ ,  $90^\circ$ ,  $135^\circ$ ).

A total of 120 features are computed, as shown in Table 1.

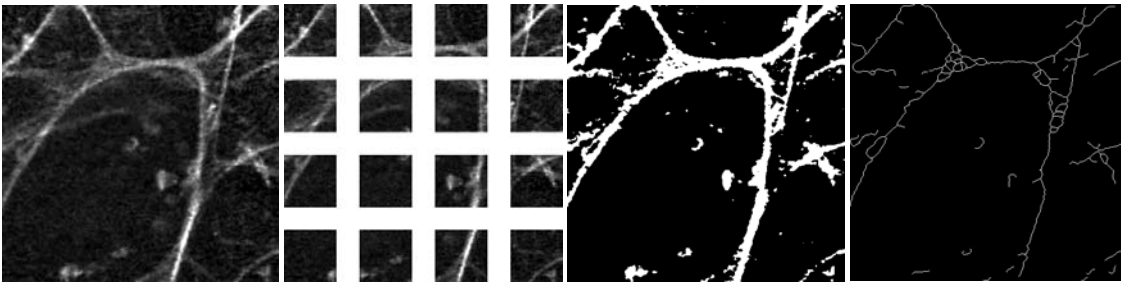


**Figure 3.** From left to right: original FCFM image, 16 subwindows, binarized image, skeleton on binarized image

**Table 1.** Features used to characterize FCFM images

	Features	Number
Contrast	Global histogram statistics	5
	Local histogram statistics	80
	Density	1
	Local densities	16
	Sum of image gradient	1
Shape	Number of junction points in skeleton	1
Texture	Haralick parameters	16
Total		120

## 2.2 Classifier

On the previously cited features several standard classifiers are implemented. First a 1-Nearest Neighbour (1-NN) classifier, which allows to assess the discriminating power of the features. Due to the high computational cost of the 1-NN classifier, we also implemented a Support Vector Machine (SVM) classifier on our features [9]. SVM is one of the most performing and most used classification algorithm. The support vector machine classifier is a binary classifier algorithm that looks for an optimal hyperplane as a decision function in a high-dimensional space. A classical choice for the kernel is the cubic polynomial kernel.

In order to improve the prediction performance of the classifier, and to provide faster and more cost-effective decision, variable selection [4] can be used. It can also provide a better understanding of which visual features discriminate the data. Support Vector Machine -Recursive Feature Elimination (SVM-RFE) is one way to perform variable selection [6]. The goal is to find a subset of size  $r$  among  $d$  variables ( $r < d$ ) which maximizes the performance of the predictor. The method is based on a sequential backward selection. One feature at a time is removed until  $r$  features are left. The removed variables are the ones that minimize the variation of the margin.

## 2.3 Experimental protocol

Because of the large difference between non-smoker and smoker images, experiments have been conducted separately on those two groups. Indeed, alveolar fluorescence imaging in smokers dramatically differs from imaging in non-smokers. Whereas FCFM exclusively images the elastin framework of the alveolar ducts in non-smokers, in smokers, tobacco-tar induced fluorescence allows to observe the alveolar walls and the presence of macrophages (cells which digest cellular debris), as shown in Figure 4.

Two databases are used for our experiments. Database1 (see Table 2) is used (i) to assess the discriminative power of the feature space through a 1-NN classifier and (ii) for learning for the SVM with feature selection. Because of the relatively small number of non-smoker and smoker images, a leave-one-out cross validation process is used, which ensures unbiased generalization error estimation. It consists in extracting one sample image from the image base for validation, the rest of the base being used for learning. Recognition rate is computed over all the samples. This cross-validation process is used for 1-NN, SVM and SVM-RFE classification.

To assess final performance of our automatic classification system, we use a database of unseen images, from both smoker and non-smoker, healthy and pathological subjects, denoted Database2, as shown in Table 2.

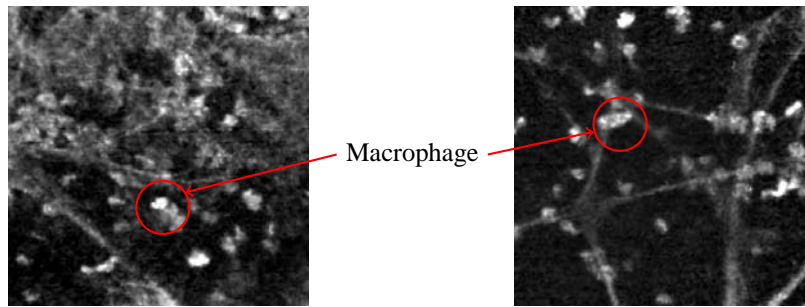


**Figure 4.** FCFM images of smoker, pathological (left) and healthy (right) cases. Notice the presence of macrophages.

**Table 2.** Number of non-smoker and smoker images in Database1 and Database2

	Non-smoker	Smoker
Healthy	35	58
Pathological	43	52
Total Database1	78	110
Healthy	10	28
Pathological	30	10
Total Database2	40	38

### 3 Results

The SVM classifier and SVM-RFE based feature selection [6] are implemented using the SVM and Kernel Methods Matlab Toolbox [1]. The system performance is assessed with correct classification rate and error rate.

**Results obtained on Database1** Results obtained with the 1-NN classifier are shown in Table 3. Let us recall that the 1-NN classifier is used here to assess the discriminative power of the feature set. As one can see in Table 3, the feature set seems to be better adapted to the discrimination of healthy/pathological non-smoker images. This can be explained by the presence of macrophages and smoke trapped in the alveolar walls in smoker images. Indeed, as one can see in Figure 5, the line network is hidden behind macrophages, making it difficult to characterize the structure. Still, recognition rates of 87% and 80% indicate that room for improvement is left with this feature set.

**Table 3.** Results obtained on Database1 provided by 1-NN classifier

		Non-smoker	Smoker
Database1	Recog. rate	87%	80%
	Error rate	13%	20%

Results obtained with the SVM and SVM-RFE are shown in Table 4. Thanks to feature selection, the number of features, initially 120, drops down to 11 for non-smoker images, and 7 for smoker images. Not surprisingly, the recognition performance achieved by the leave-one-out SVM-RFE are near 100% (i.e. 99% for non-smokers and 98% for smokers), since one can consider that this wrapper-based feature selection has been performed on the training database. The selection of relevant variables allows to gain some insight about the usefulness of features: the most discriminating ones are features computed from co-occurrence matrices, local densities, and local histogram statistics, which highlights the importance of local, contrast-based differences between healthy and pathological subjects.

**Results obtained on Database2** To assess the final performance of our classification system, SVM in 120-feature space and SVM in reduced feature space (11 for non-smoker subjects and 7 for smoker subjects) are compared on Database2 (see Table 4). Let us recall that this database includes images that have not been seen during training. Therefore, one can consider that results obtained on Database2 are somehow predictive of the behaviour of our classification system. One can also observe that classification accuracy has not been significantly decreased (even increased for non-smoker



**Figure 5.** FCFM images of a smoker with pathology, showing how the line network is hidden behind the macrophages. Network is manually highlighted by an expert on the right image.

**Table 4.** Results obtained on Database1 and Database2 provided by SVM and SVM-RFE classifier

		Non-smoker		Smoker	
		SVM	SVM-RFE	SVM	SVM-RFE
	Feature number	120	11	120	7
Database1	Recog. rate	88%	99%	93%	98%
	Error rate	12%	1%	7%	2%
Database2	Recog. rate	75%	78%	87%	84%
	Error rate	25%	22%	13%	16%

images) while greatly reducing the size of the feature space, thus bringing some new interesting future work about the representation of FCFM images.

## 4 Conclusions

The present work deals with the classification of a new category of images from the distal lung. The images were acquired using a fibered confocal fluorescence microscopy, a technique that enables the observation of in vivo alveolar structures for the first time. Such images are not well described so far and are difficult to discriminate by pathologists and respiratory physicians. Our classification system, that aims at discriminating healthy cases from pathological ones, shows satisfying performance for non-smoker and smoker images. However, the current database should be extended to confirm these results. Because the clinical trial is ongoing, this will be feasible in the near future. Future work will concern rendering the process real-time, so as to aid the clinician during examination in real time. Classification methods could also give information about which part of the image is the most discriminant or which part of the structure might be more altered by pathologies. A future goal will also be to discriminate between different pathologies: interstitial lung diseases (abestosis, systemic sclerosis, fibrosis, sarcoidosis), carcinomatous lesions etc.

## References

1. S. Canu, Y. Grandvalet, V. Guigue and A. Rakotomamonjy: "SVM and Kernel Methods Matlab Toolbox", *Perception Systèmes et Information, INSA de Rouen, Rouen, France, 2005.*
2. G.S. Dibajaa and E. Thiel: "Skeletonization algorithm running on path-based distance maps", *Image and Vision Computing*, vol.14, p.47-57, 1996.
3. R.O. Duda and P.E. Hart: "Pattern Classification and Scene Analysis," *John Wiley & Sons, 1973.*
4. I. Guyon and A. Elisseeff: "An introduction to variable and feature selection", *Journal of Machine Learning Research*, vol.3, p.1157-1182, 2003.
5. R.M. Haralick, K. Shanmugam and I. Dinstein: "Textural Features for Image Classification," *Systems, Man and Cybernetics*, vol.3, no.6, p.610-621, 1973.
6. A. Rakotomamonjy: "Variable selection using SVM-based criteria," *Journal of Machine Learning Research*, 3:1357-1370, 2003.
7. L. Thiberville, S. Moreno-Swirc, T. Vercauteren, E. Peltier, C. Cave and G. Bourg-Heckly: "In vivo imaging of the bronchial wall microstructure using fibered confocal uorescence microscopy," *American Journal of Respiratory and Critical Care Medicine*, vol.175, no.1, p.22-31, 2007.
8. L. Thiberville, G.Bourg-Heckly, M. Salaün, S. Dominique and S. Moreno-Swirc: "Human in-vivo confocal microscopic imaging of the distal bronchioles and alveoli," *Chest Journal*, vol.132, no.4, p.426, 2007.
9. V. Vapnik: "The nature of statistical learning theory," *Springer, 1995.*